

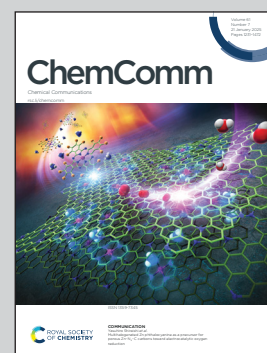
Showcasing research from Professor Sudipta Roy's laboratory, Department of Chemistry, Indian Institute of Science Education and Research (IISER) Tirupati, Andhra Pradesh, India.

Isolation of mixed valence charge-neutral Ag<sub>12</sub>, and dicationic Ag<sub>10</sub> nano-clusters stabilized by carbene-phosphaalkenides

Cyclic alkyl(amino) carbene-supported phosphaalkenides were employed as ligands for isolation of two atomically precise mixed-valence nanoclusters (NCs) with Ag<sub>12</sub><sup>0</sup>Cl<sub>3</sub>, and Ag<sub>10</sub><sup>2+</sup> cores. The characteristic EPR signals exhibited by the NCs suggested coupling of unpaired electrons with <sup>35,37</sup>Cl, <sup>31</sup>P and <sup>107,109</sup>Ag nuclei.

The cover image was prepared using components from  
© Natalia Dobrovolska | Dreamstime.com.

As featured in:



See Sudipta Roy *et al.*,  
*Chem. Commun.*, 2025, **61**, 1379.



Cite this: *Chem. Commun.*, 2025, 61, 1379

Received 23rd October 2024,  
Accepted 11th December 2024

DOI: 10.1039/d4cc05628k

rsc.li/chemcomm

# Isolation of mixed valence charge-neutral Ag<sub>12</sub>, and dicationic Ag<sub>10</sub> nano-clusters stabilized by carbene-phosphaalkenides†

Maria Francis, <sup>a</sup> Asutosh Patra, <sup>a</sup> Farsana Abdul Salam, <sup>a</sup> Siriya Jagannatha Prathapa<sup>b</sup> and Sudipta Roy <sup>\*,a</sup>

Cyclic alkyl(amino) carbene (cAAC)-supported phosphaalkenides (cAAC=P)<sup>−</sup> have been employed as ligands for the isolation of two atomically precise mixed valence paramagnetic Ag<sub>12</sub><sup>I/0</sup>Cl<sub>3</sub>, and Ag<sub>10</sub><sup>I/0</sup>, nano-clusters [(Me<sub>2</sub>-cAAC=P)<sub>6</sub>Ag<sub>12</sub>Cl<sub>3</sub>] (2), and [(Me<sub>2</sub>-cAAC=P)<sub>6</sub>Ag<sub>10</sub>](NTf<sub>2</sub>)<sub>2</sub> (4). 2 and 4 have been structurally characterized by single-crystal X-ray diffraction revealing the presence of three Ag<sup>0</sup> atoms, nine Ag<sup>I</sup> ions (2); and two Ag<sup>0</sup> atoms, eight Ag<sup>I</sup> ions (4), respectively. The clustering inorganic unit Ag<sub>12</sub>Cl<sub>3</sub> in 2 has been found to be surrounded by six mono-anionic μ<sub>3</sub>-cAAC=P moieties having 3-bar symmetry. 2 and 4 have been studied by cyclic voltammetry, UV-vis, ESI-MS, XPS, EPR spectroscopy, and DFT calculations.

Silver nanoclusters (NCs) are known to exhibit unique electronic, and optical properties, such as strong photoluminescence, and various catalytic activities.<sup>1</sup> They are utilised as attractive luminescent probes for sensing and bioimaging.<sup>2</sup> Structurally well-defined NCs possessing Ag<sup>0</sup> atoms are highly reactive, and easier to oxidize compared to their heavier Au analogues, which makes their synthesis challenging. Metallic silver is non-magnetic in its bulk form. However, Pereiro *et al.* theoretically predicted that the small nuclearity silver NCs, Ag<sub>n</sub>, could be magnetic with variation of the magnetic moment depending on the value of *n* [*n* = 2–22].<sup>3</sup> Liu *et al.* reported the isolation of the chiral open-shell Ag<sub>23</sub> NC with five Ag<sup>0</sup> atoms, which was structurally characterized by single-crystal X-ray diffraction.<sup>4</sup> The open-shell behaviour of this Ag<sub>23</sub> NC was confirmed by a weak electron paramagnetic resonance (EPR) signal, characteristic of *s* = 1/2, with *g* = 1.959 and 1.955.<sup>4</sup> The first atomically precise mixed valence Ag<sub>22</sub><sup>0/I</sup> NC displaying thermally activated delayed fluorescence (TADF) was reported in 2022 by Sun and

co-workers.<sup>5</sup> In the same year, two other mixed valence NCs Ag<sub>8</sub><sup>0/I</sup> and Ag<sub>29</sub><sup>0/I</sup> exhibiting strong EPR signals were reported.<sup>6</sup> The heavily Ag<sup>0</sup>-doped KCl:AgCl crystals in different chemical defect positions [cationic and anionic holes] were studied by EPR spectroscopy.<sup>7a</sup> The generation of Ag<sub>4</sub><sup>3+</sup>, and Ag<sub>6</sub><sup>+</sup> clusters was also reported under different chemical conditions.<sup>7b,c</sup> However, the mixed valence silver NCs are rarely reported.<sup>8</sup> The first closed-shell mixed valence Ag<sub>2</sub><sup>I/III</sup> [Ag⋯Ag 7.4 Å] containing N<sub>8</sub>-donor macrocyclic ligand was isolated by Qin-Hui *et al.* in 1994.<sup>9a</sup> The 1D zig-zag chain of Ag<sub>2</sub><sup>I/II</sup> (ref. 9b) stabilized by the cyclic alkyl(amino) carbene (cAAC)-supported mono-anion of the inversely polarized phosphaalkene, *viz.*, the phosphaalkenide<sup>10</sup> was reported by Roy and co-workers. N-heterocyclic carbene (NHC), and P-SiMe<sub>3</sub> ligated diamagnetic Ag<sub>12</sub><sup>I</sup>, and Ag<sub>26</sub><sup>I</sup> clusters were reported by Corrigan *et al.*<sup>11</sup> A plethora of other Ag<sup>I</sup> clusters have been synthesized, and characterized employing alkyne, thiolate, sulfide, selenide, phosphine, perchlorate, *etc.* as ligands.<sup>12</sup> Moreover, clusters with Ag–H moieties have also been isolated, and further studied by mass spectrometry.<sup>13</sup> However, isolation of stable silver NCs introducing carbene-phosphaalkenides as ligands is still scarce. Herein, we report on the solid-state isolation, and structural characterization of two novel structurally well-defined mixed valence paramagnetic silver NCs with Ag<sub>12</sub><sup>I/0</sup>Cl<sub>3</sub>, and Ag<sub>10</sub><sup>I/0</sup> metallic cores.

The dark red crystals of Me<sub>2</sub>-cAAC=P–K (1)<sup>14</sup> (Me<sub>2</sub>-cAAC=C(N-2,6-<sup>i</sup>Pr<sub>2</sub>C<sub>6</sub>H<sub>3</sub>)(CMe<sub>2</sub>)<sub>2</sub>(CH<sub>2</sub>)) were reacted with AgNTf<sub>2</sub> in a 3 : 2 molar ratio in toluene at 0 °C to room temperature (rt) for 12 h to obtain a dark brown-red reaction mixture. Upon drying, the resultant crystalline solid obtained was dissolved in freshly distilled DCM, and stored for crystallization upon concentration to ~1 mL in a freezer at −40 °C. After one-week, dark red blocks of [(Me<sub>2</sub>-cAAC=P)<sub>6</sub>(Ag)<sub>12</sub>(Cl)<sub>3</sub>] (2) were isolated in 40% yield (Scheme 1). The presence of the three chloride ions in 2 can be attributed to the decomposition of DCM, the usage of which is found to be crucial for the isolation of 2. A different mixed valence dicationic cluster [(Me<sub>2</sub>-cAAC=P)<sub>6</sub>(Ag)<sub>10</sub>](NTf<sub>2</sub>)<sub>2</sub> (4) was isolated in 60% yield as yellow blocks when [Me<sub>2</sub>-cAAC=P–B(N(<sup>i</sup>Pr)<sub>2</sub>)<sub>2</sub>] (3)<sup>9b</sup> was reacted with AgNTf<sub>2</sub> in 2 : 1

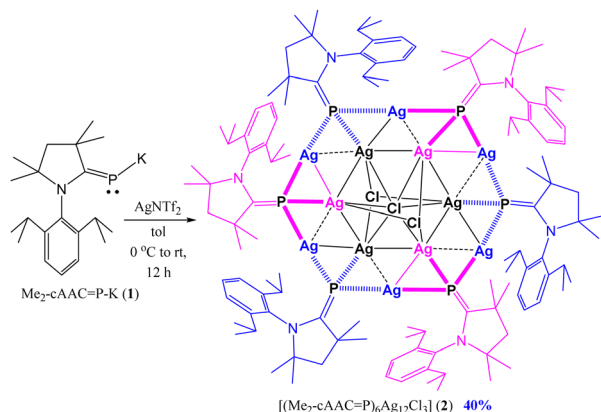
<sup>a</sup> Department of Chemistry, Indian Institute of Science Education and Research (IISER) Tirupati, Tirupati 517619, India. E-mail: roy.sudipta@iisertirupati.ac.in

<sup>b</sup> Bruker India Scientific Pvt. Ltd, India

† Electronic supplementary information (ESI) available. CCDC 2242239 (2), 2194453 (4). For ESI and crystallographic data in CIF or other electronic format see DOI: <https://doi.org/10.1039/d4cc05628k>

‡ Both authors contributed equally.





Scheme 1 Synthesis of mixed-valence neutral NC  $[(\text{Me}_2\text{-cAAC}=\text{P})_6\text{Ag}_{12}(\text{Cl})_3]$  (**2**).

molar ratio in toluene at rt for 12 h, followed by crystallization of the resultant precipitate from concentrated DCM solution, stored at 0 °C in a refrigerator (Scheme 2). The  $(\text{cAAC}=\text{P})^-$  ligands are found to be redox non-innocent, and undergo oxidation to produce the corresponding radical followed by dimerization, resulting in the formation of  $(\text{Me}_2\text{-cAAC})_2\text{P}_2$  with a subsequent reduction of  $\text{Ag}^{\text{I}}$  to  $\text{Ag}^0$  in solution affording the mixed valence Ag-NCs **2** and **4**.<sup>6</sup> The presence of  $\text{Ag}^0$  and  $\text{Ag}^{\text{I}}$  centres in **2** and **4** is supported by XPS spectroscopy (see ESI†). The formation of  $(\text{Me}_2\text{-cAAC})_2\text{P}_2$  in the reaction mixture is confirmed by  $^{31}\text{P}$  NMR spectroscopy ( $\delta = 55.1$  ppm).

The red/yellow blocks of **2/4** are found to be stable under an argon atmosphere for six months inside a glove box at rt. The powders of **2** and **4** decompose above 205 and 165 °C, respectively. **2** and **4** are found to be NMR silent, and EPR active.

**2** and **4** have been structurally characterized by single-crystal X-ray diffraction. The dodeca-nuclear Ag-NC  $[(\text{Me}_2\text{-cAAC}=\text{P})_6(\text{Ag})_{12}(\text{Cl})_3]$  (**2**) crystallizes in the trigonal  $R\bar{3}$  space group (Fig. 1). **2** comprises six  $(\text{Me}_2\text{-cAAC}=\text{P})^-$  ligands, three chloride ions, and twelve Ag-atoms/ions. Fig. 2 shows that the asymmetric unit of **2** starting at position-1, generates six different symmetry equiv. points (1–6). Positions 1, 3 and 5 are non-inverted, while positions 2, 4 and 6 are three inverted-symmetry equiv. positions. There are three  $\text{Ag}^0$  atoms in **2**, which is

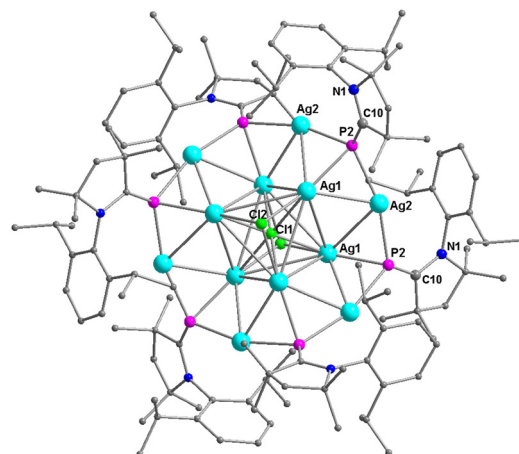


Fig. 1 Molecular structure of NC  $[(\text{Me}_2\text{-cAAC}=\text{P})_6(\text{Ag})_{12}(\text{Cl})_3]$  (**2**). Hydrogen atoms are omitted for clarity.

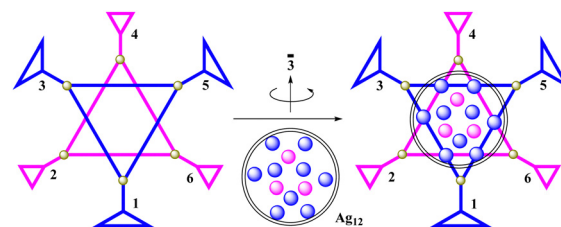
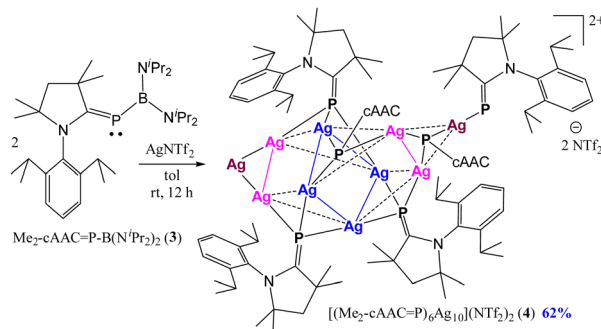


Fig. 2 Structural topology and symmetry  $[3\text{-bar}]$  in NC **2**.

suggested from charge balance consideration, since there are a total of nine mono-anionic ligands present.

The space filling model of **2** has been shown in Fig. 3 (left), which represents how the central  $\text{Ag}_{12}$  metallic core is well protected by the surrounding cAAC-supported phosphaaikenide ligands. The natural bond orbital (NBO) analyses of NCs **2** and **4** at neutral doublet, and dicationic triplet states, respectively, were performed at the UBP86-D3(BJ)/Def2-SVP level of theory (see ESI† for details). The NBO analysis of **2** revealed that the  $\alpha\text{-LUMO}+1$ ,  $\alpha\text{-LUMO}$ , and  $\alpha\text{-SOMO}$  are very close in energy ( $\Delta E = 0.01\text{--}0.05$  eV) suggesting that the unpaired electron in **2** can span all these three orbitals involving the  $\text{C}=\text{N}-\text{P}$  unit, Cl and Ag atoms (see ESI†). This is also reflected in the Mulliken  $\alpha$ -spin densities of **2** showing delocalization of spin densities due to the unpaired electron (Fig. 3 (right), see ESI†).

The Ag–Ag distances of charge-neutral NC **2** are found to be 2.883(1), and 3.024(2) Å, which are significantly shorter than



Scheme 2 Synthesis of mixed-valence dicationic NC  $[(\text{Me}_2\text{-cAAC}=\text{P})_6\text{Ag}_{10}](\text{NTf}_2)_2$  (**4**).

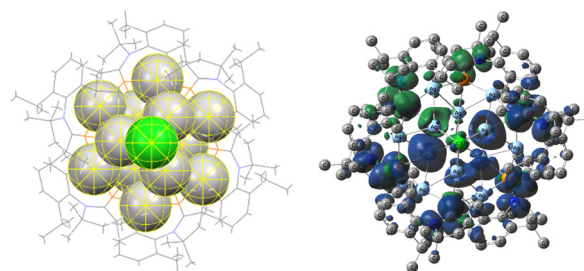


Fig. 3 Space filling model (left), and Mulliken  $\alpha$ -spin densities (right) of  $[(\text{Me}_2\text{-cAAC}=\text{P})_6\text{Ag}_{12}\text{Cl}_3]$  (**2**).





those of the previously isolated tri-cationic closed-shell Ag NC  $2^{3+}(\text{OTf}^-)_3$  (2.9593(14), 2.9174 (12), 3.2026(15), 3.1541(13) Å).<sup>6</sup> The Ag–P distances of **2** are 2.379(4), 2.401(3), and 2.455(2) Å, which are close to those of  $2^{3+}(\text{OTf}^-)_3$  (Ag–P 2.393(4)–2.431(4) Å).<sup>6</sup> The C–P bond in **2** is 1.75(1) Å, which is slightly shorter than those of  $2^{3+}(\text{OTf}^-)_3$  (1.780(11)–1.801(11) Å).<sup>6</sup> The Ag–Cl distances in **2** are found to be 2.4530(14), and 2.572(7) Å, which are either very similar in value or significantly smaller than those of  $2^{3+}$  (2.475(9), 2.705(5), 2.638 (4), 2.7143(11), 2.732(4), 2.8254(10) Å).<sup>6</sup> The diameter of the outer/peripheral Ag<sub>6</sub> ring of **2** having a three-fold symmetry is 8.37 Å, which is very close to those of  $2^{3+}$  with two-fold symmetry (8.26, 8.36, 8.48 Å).<sup>6</sup> The Cl–Cl distance between the two extreme Cl-ions in **2** is 5.8 Å, which is shorter than that of  $2^{3+}$  (6.5 Å).<sup>6</sup> The P–P distance in **2** is 9.02 Å, which is slightly greater than the average value of  $2^{3+}$  (8.46 Å; 8.26, 8.36, 4.48, 8.88, 9.22 Å).<sup>6</sup> **2** represents the first example of an Ag<sup>I/0</sup> based mixed valence NC, which has been structurally characterized in two different charged (0 (**2**) vs. +3 ( $2^{3+}$ )), and spin states [doublet (**2**) vs. singlet ( $2^{3+}$ )].<sup>6</sup>

The dicationic deca-nuclear Ag NC [(Me<sub>2</sub>-cAAC=P)<sub>6</sub>Ag<sub>10</sub>](NTf<sub>2</sub>)<sub>2</sub> (**4**) crystallizes in triclinic space group *P* $\bar{1}$  (Fig. 4). The entire molecule of **4** appears in the crystallographic asymmetric unit, which possesses six mono-anionic ligands (Me<sub>2</sub>-cAAC=P)<sup>−</sup>, and ten Ag-atoms/ions. There are two non-coordinating/free mono-anionic NTf<sub>2</sub><sup>−</sup> anions present for the electrical charge balance. The charge balance consideration suggests that there are two Ag<sup>0</sup> atoms in **4**. The four arms of the central Ag<sub>4</sub> unit of **4** have been bridged by four P-atoms of mono-anionic Me<sub>2</sub>-cAAC=P<sup>−</sup> ligands producing a (Me<sub>2</sub>-cAAC=P)<sub>4</sub>Ag<sub>4</sub> unit. Two Ag<sub>2</sub> units have been placed in anti-fashion above and below the irregular square-like Ag<sub>4</sub> unit (Fig. 4 and 5).

An additional Ag-atom is present above the Ag<sub>2</sub> unit (Fig. 4 and 5), while another Ag atom is bridged by a μ<sub>3</sub>-P atom (right, Fig. 5). The Ag–Ag distances of the central four-membered Ag<sub>4</sub> ring in **4** are 2.90, 3.0, and 3.20 Å, which are longer than those (~2.96 Å) of the Ag<sub>8</sub><sup>0/I</sup> complex.<sup>6</sup>

The Ag<sub>2</sub> unit, which is situated on the top of the central Ag<sub>4</sub> unit, possesses the Ag–Ag distance of 2.91 Å, which is

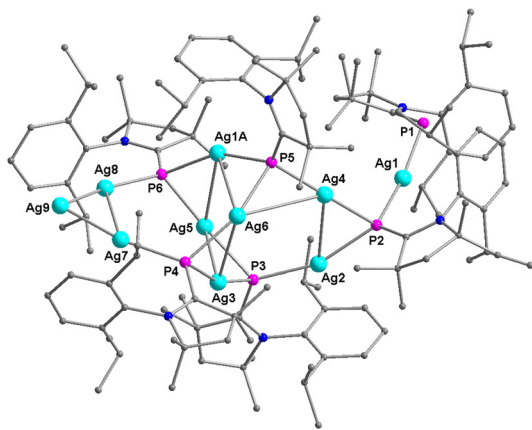


Fig. 4 Molecular structure of NC [(Me<sub>2</sub>-cAAC=P)<sub>6</sub>Ag<sub>10</sub>](NTf<sub>2</sub>)<sub>2</sub> (**4**). Hydrogen atoms are omitted for clarity. Two triflimide anions [N(SO<sub>2</sub>CF<sub>3</sub>)<sub>2</sub>]<sup>−</sup> are omitted for clarity.

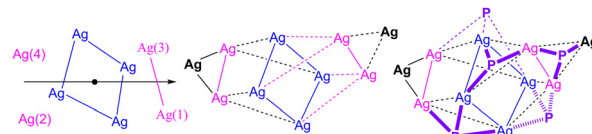


Fig. 5 Core topology of [(Me<sub>2</sub>-cAAC=P)<sub>6</sub>Ag<sub>10</sub>](NTf<sub>2</sub>)<sub>2</sub> (**4**). Two Ag<sub>6</sub> square prisms sharing the blue colored pseudo-Ag<sub>4</sub>-square with a 4-bar symmetry operation.

significantly shorter than that of the Ag<sub>3</sub> triangle of **4** (3.04 Å). The corresponding Ag–Ag distance in previously reported Ag<sub>8</sub><sup>0/I</sup> complexes is 3.07 Å.<sup>6</sup> Notably, the distal Ag atom (Ag9) (Ag7–Ag9, Ag8–Ag9; 2.472(3), 2.458(3) Å) is significantly closer to the Ag<sub>2</sub> arm (Ag8–Ag9), which is situated above the central Ag<sub>4</sub> unit of **4**. The Ag–P bond lengths of NC Ag<sub>10</sub><sup>0/I</sup> (**4**) range from 2.23 Å to 2.48 Å, and are significantly different than those of the neutral Ag<sub>8</sub> cluster (2.404(5)–2.417(4) Å).<sup>6</sup> The space filling diagram of a ten Ag atoms/ions unit of **4** has been shown in Fig. 6 (left). The Ag atom placed above the Ag<sub>2</sub> unit is situated in between the two aromatic rings of the Dipp ligands. The NBO, and Mulliken spin density analyses of **4** (Fig. 6 (right)) showed the major spin densities on the C=N–P unit with very small values on the Ag-atoms except for one Ag-atom (5.6%) and thus typical EPR features of Ag–P systems were not observed<sup>6</sup> in the experimental EPR spectrum of **4**.

The EPR spectra of **2** and **4** (in DCM) are shown in Fig. 7 and 8. The EPR simulation/fitting of **2** considering coupling of the unpaired electron with the nuclei of <sup>107,109</sup>Ag, <sup>31</sup>P and <sup>35,37</sup>Cl atoms is quite satisfactory (Fig. 7). Three board lines near *g* = 2.0033 were observed for the previously reported Ag<sub>8</sub><sup>0/I</sup> cluster containing four Ag<sup>0</sup> atoms.<sup>6,9b</sup> However, the EPR spectrum of **2** shows three sets of multiple hyperfine lines, which have been simulated with EasySpin.

The coupling constants of one <sup>107,109</sup>Ag<sup>0</sup>, two <sup>31</sup>P and one <sup>35,37</sup>Cl nuclei are 9.43, 111.79/111.75, and 9.81 MHz, respectively, with a slight rhombic nature of *g* [*g*<sub>x</sub> = 2.00766, *g*<sub>y</sub> = 2.00885, *g*<sub>z</sub> = 1.99959]. The EPR spectrum of **4** appears as unsymmetrical showing two resonances around *g* ≈ 2 [*g*<sub>x</sub> = 2.00165, *g*<sub>y</sub> = 2.00006, *g*<sub>z</sub> = 1.99703] (Fig. 8). The coupling constant of Ag<sup>0</sup> is 2.51 MHz, which is significantly smaller than that of **2** (9.43 MHz). The ESI-MS studies show that **2** (see ESI<sup>†</sup>) and **4** can fly as dications. The ESI-MS spectrum of **4**<sup>2+</sup> corroborates the loss of two isopropyl groups with the intake of a sodium ion as [(Me<sub>2</sub>cAACP)<sub>6</sub>Ag<sub>10</sub> + Na–2C<sub>3</sub>H<sub>7</sub>–H]<sup>2+</sup>. The cyclic

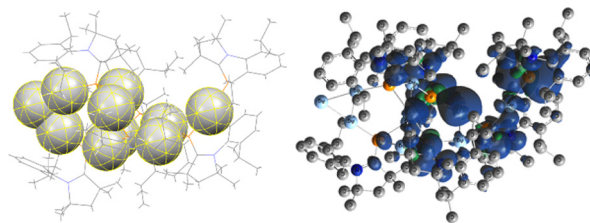


Fig. 6 Space filling model of total molecule (left), and Mulliken  $\alpha$ -spin densities (right) of [(Me<sub>2</sub>-cAAC=P)<sub>6</sub>Ag<sub>10</sub>](NTf<sub>2</sub>)<sub>2</sub> (**4**).



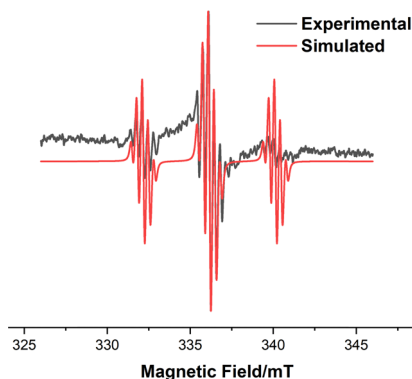


Fig. 7 Experimental (black), and simulated (red) X-band EPR spectra of  $[(\text{Me}_2\text{-cAAC}=\text{P})_6(\text{Ag})_{12}(\text{Cl}_3)]$  (**2**) in DCM at 293 K. EasySpin, simulated parameters: one  $^{107,109}\text{Ag}(0)$  [ $A = 9.43$  MHz], two  $^{31}\text{P}$  [ $A = 111.79$ ,  $111.75$  MHz], one  $^{35,37}\text{Cl}$  [ $A = 9.81$  MHz],  $g_x = 2.00766$ ,  $g_y = 2.00885$ ,  $g_z = 1.99959$ ,  $\text{LW1} = 0.016$  mT,  $\text{LW2} = 0.166$  mT. Experimental frequency =  $9.436369$  GHz.

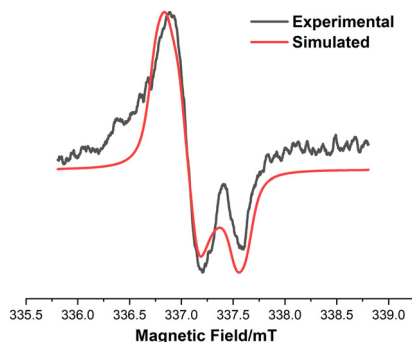


Fig. 8 X-band EPR spectrum of the NC  $[(\text{Me}_2\text{-cAAC}=\text{P})_6(\text{Ag})_{10}](\text{NTf}_2)$  (**4**) in DCM at 293 K. Black line represents the experimental spectrum, and the red line represents the simulated spectrum using the EasySpin program [ $g_x = 2.00165$ ,  $g_y = 2.00006$ ,  $g_z = 1.99703$ ,  $\text{LWPP1} = 0.0678384$  mT,  $\text{LWPP2} = 0.0817786$  mT,  $A_{\text{Ag}} = 2.51891$  MHz].

voltammetry studies of **2** and **4** suggest the possible oxidation (see ESI†). The UV-vis spectra (in THF at 298 K) of **2** and **4** exhibited the absorption maxima ( $\lambda_{\text{max}}$ ) at 365 and 367 nm, respectively (see ESI†). **2** and **4** were observed to be non-emissive.

In conclusion, two novel mixed valence Ag-NCs ( $\text{Ag}_{10}$ , **2**;  $\text{Ag}_{12}$ , **4**) were isolated as red/yellow blocks. **2** and **4** have been structurally characterized by X-ray single-crystal diffraction. The  $\text{Ag}_{10}$ , and  $\text{Ag}_{12}$  NCs possess three and two  $\text{Ag}^0$  atoms, respectively. The NMR silent NCs **2** and **4** were found to be EPR active. The unpaired electrons couple with the  $^{35,37}\text{Cl}$ ,  $^{31}\text{P}$  and  $^{107,109}\text{Ag}$  nuclei. The strongest coupling constant was obtained for  $^{31}\text{P}$ -nuclei (111.75 MHz) in **2**. The coupling constant of  $^{107,109}\text{Ag}$  of **2** (9.43 MHz) is four times stronger than that of **4** (2.51 MHz). The distributions of electron densities in **2** and **4** were estimated by computation of the Mulliken spin densities, and further correlated with ERP simulation.

SR gratefully acknowledges STARS-IISC, MoE (MoE-STARS/STARS-2/2023-0666), IISERT, CSIR for the generous financial

support. We thank Dr S. S. Sen (NCL-Pune), and KB for the XPS measurements.

## Data availability

The data supporting this article (experimental details, UV-vis, HRMS, EPR, XPS, single-crystal X-ray data, and computational details) have been included as part of the ESI†. Crystallographic data for **2** and **4** have been deposited at the CCDC (2242239, 2194453†), and can be obtained from <https://www.ccdc.cam.ac.uk/>.

## Conflicts of interest

There are no conflicts to declare.

## Notes and references

- (a) C. M. Aikens, *J. Phys. Chem. Lett.*, 2011, **2**, 99; (b) Y. Du, H. Sheng, D. Astruc and M. Zhu, *Chem. Rev.*, 2020, **120**, 526.
- (a) T. Udayabhaskararao and T. Pradeep, *J. Phys. Chem. Lett.*, 2013, **4**, 1553; (b) K. Zheng, X. Yuan, N. Goswami, Q. Zhang and J. Xie, *RSC Adv.*, 2014, **4**, 60581.
- M. Pereiro, D. Baldomir and J. E. Arias, *Phys. Rev. A*, 2007, **75**, 063204.
- C. Liu, T. Li, H. Abroshan, Z. Li, C. Zhang, H. J. Kim, G. Li and R. Jin, *Nat. Commun.*, 2018, **9**, 744.
- Z.-R. Yuan, Z. Wang, B.-L. Han, C.-K. Zhang, S.-S. Zhang, Z.-Y. Zhu, J.-H. Yu, T.-D. Li, Y.-Z. Li, C.-H. Tung and D. Sun, *Angew. Chem., Int. Ed.*, 2022, **61**, e202211628.
- E. Nag, S. Battuluri, K. C. Mondal and S. Roy, *Chem. – Eur. J.*, 2022, **28**, e202202324.
- (a) P. G. Baranov, N. G. Romanov, V. A. Khramtsov and V. S. Vikhnin, *J. Phys.: Condens. Matter*, 2001, **13**, 2651; (b) J. Sadlo, J. Michalik and L. Kevan, EPR and ESEEM study of silver clusters in ZK-4 molecular sieves, *Nukleonika*, 2006, **51**, 49; (c) A. Baldansuren, R. Eichel and E. Roduner, *Phys. Chem. Chem. Phys.*, 2009, **11**, 6664.
- H. Hirai, S. Ito, S. Takano, K. Koyasu and T. Tsukuda, *Chem. Sci.*, 2020, **11**, 12233.
- (a) Y. Shu-Yan, L. Qin-Hui and S. Meng-Chang, *Inorg. Chem.*, 1994, **33**, 1251; (b) E. Nag, S. Battuluri, B. B. Sinu and S. Roy, *Inorg. Chem.*, 2022, **61**, 3007.
- L. Weber, U. Lassahn, H.-G. Stammel and B. Neumann, *Eur. J. Inorg. Chem.*, 2005, 4590.
- B. K. Najafabadi and J. F. Corrigan, *Chem. Commun.*, 2014, **51**, 665.
- (a) D. Fenske and F. Simon, *Angew. Chem., Int. Ed. Engl.*, 1997, **36**, 230; (b) X. He, H.-X. Liu and L. Zhao, *Chem. Commun.*, 2016, **52**, 5682; (c) X.-J. Wang, T. Langetepe, C. Persau, B.-S. Kang, G. M. Sheldrick and D. Fenske, *Angew. Chem., Int. Ed.*, 2002, **41**, 3818; (d) D. Fenske, C. Persau, S. Dehnen and C. E. Anson, *Angew. Chem., Int. Ed.*, 2004, **43**, 305; (e) M. Ueda, Z. L. Goo, K. Minami, N. Yoshinari and T. Konno, *Angew. Chem., Int. Ed.*, 2019, **58**, 14673; (f) Z.-A. Nan, Y. Wang, Z.-X. Chen, S.-F. Yuan, Z.-Q. Tian and Q.-M. Wang, *Chem. Commun.*, 2018, **1**, 1; (g) J.-W. Liu, H.-F. Su, Z. Wang, Y.-A. Li, Q.-Q. Zhao, X.-P. Wang, C.-H. Tung, D. Sun and L.-S. Zheng, *Chem. Commun.*, 2018, **54**, 4461; (h) L. G. AbdulHalim, M. S. Bootharaju, Q. Tang, S. Del Gobbo, R. G. AbdulHalim, M. Eddaoudi, D.-E. Jiang and O. M. Bakr, *J. Am. Chem. Soc.*, 2015, **137**, 11970; (i) S.-F. Yuan, Z.-J. Guan, W.-D. Liu and Q.-M. Wang, *Nat. Commun.*, 2019, **10**, 1; (j) C. Sun, B. K. Teo, C. Deng, J. Lin, G.-G. Luo, C.-H. Tung and D. Sun, *Coord. Chem. Rev.*, 2021, **427**, 213576; (k) M. S. Bootharaju, R. Dey, L. E. Gevers, M. N. Hedhili, J.-M. Basset and O. M. Bakr, *J. Am. Chem. Soc.*, 2016, **138**, 13770.
- M. Jash, A. C. Reber, A. Ghosh, D. Sarkar, M. Bodiuzzaman, P. Basuri, A. Baksi, S. N. Khanna and T. Pradeep, *Nanoscale*, 2018, **10**, 15714.
- A. Kulkarni, S. Arumugam, M. Francis, P. G. Reddy, E. Nag, S. M. N. V. T. Gorantla, K. C. Mondal and S. Roy, *Chem. – Eur. J.*, 2021, **27**, 200.

